Dosimetry characterization of ^{32}P intravascular brachytherapy source wires using Monte Carlo codes PENELOPE and GEANT4

Javier Torres and Manuel J. Buades
Servicio de Radiofísica y Protección Radiológica, Hospital Universitario "Virgen de la Arrixaca," E-30120 Murcia, Spain

Julio F. Almansa and Rafael Guerrero
Servicio de Radiofísica y Protección Radiológica, Hospital Universitario "Puerta del Mar," E-11009 Cádiz, Spain

Antonio M. Lallena[a)]
Departamento de Física Moderna, Universidad de Granada, E-18071 Granada, Spain

(Received 20 May 2003; revised 10 October 2003; accepted for publication 12 November 2003; published 23 January 2004)

Monte Carlo calculations using the codes PENELOPE and GEANT4 have been performed to characterize the dosimetric parameters of the new 20 mm long catheter-based ^{32}P beta source manufactured by the Guidant Corporation. The dose distribution along the transverse axis and the two-dimensional dose rate table have been calculated. Also, the dose rate at the reference point, the radial dose function, and the anisotropy function were evaluated according to the adapted TG-60 formalism for cylindrical sources. PENELOPE and GEANT4 codes were first verified against previous results corresponding to the old 27 mm Guidant ^{32}P beta source. The dose rate at the reference point for the unsheathed 27 mm source in water was calculated to be 0.215 ± 0.001 cGy s^{-1} mCi^{-1}, for PENELOPE, and 0.2312 ± 0.0008 cGy s^{-1} mCi^{-1}, for GEANT4. For the unsheathed 20 mm source, these values were 0.2908 ± 0.0009 cGy s^{-1} mCi^{-1} and 0.311 ± 0.001 cGy s^{-1} mCi^{-1}, respectively. Also, a comparison with the limited data available on this new source is shown. We found non-negligible differences between the results obtained with PENELOPE and GEANT4. © *2004 American Association of Physicists in Medicine.* [DOI: 10.1118/1.1637970]

Key words: intravascular brachytherapy, Monte Carlo simulation, ^{32}P

I. INTRODUCTION

One of the major limitations of coronary interventions lies in the appearance of restenosis of the treated vessel. Restenosis occurs in 35%–40% of the treated patients in the case of angioplasty, while the percentage reduces to 22%–32% in case coronary stents are used.[1]

Intravascular brachytherapy appears to be a useful tool to solve such problems.[2] PREVENT[3] and INHIBIT[4] studies have pointed out the ability of ionizing radiation to inhibit restenosis. Though either gamma and beta radiation have been used, endovascular beta radiotherapy has become most popular in Europe due to the obvious radiation safety advantages.

This new, rapidly growing interest has led both the AAPM[5] and the ESTRO[6] to report recommendations on the medical physic issues. At the minimum standard level, the dose at the prescription point in the central plane is encouraged to be recorded and reported. Additional dose calculations in peripheral planes require complete two-dimensional (2-D) dosimetry information. However, beta sources present a high dose gradient, the distances in which the dose is deposited being considerably small. This has made it difficult to perform adequate dosimetry on intravascular sources.

Recently, the dosimetric characterization of a 27 mm long, catheter-based, ^{32}P beta source wire, manufactured by Guidant Corporation (Houston, TX), has been done by means of a plastic scintillator[7] and radiochromic film.[7,8]

Monte Carlo (MC) simulations have proved to be a valuable complementary means for determining the dose distributions around beta emitters. The ^{32}P source mentioned above has been simulated with different MC codes (MCNPv4B2,[7–10] CYLTRAN/ITS3,[7,11] MCNPv4C,[7] EGS4,[9,12,13] and EGSnrc[12]) and the calculated doses agree to within <10% with the experimental results.

In this work we address the 2-D dosimetric characterization of a new, clinically used, 20 mm long catheter-based ^{32}P beta source wire, commercially available in the Galileo™ Intravascular Radiotherapy System, manufactured also by the Guidant Corporation. This source has been used[14] in a detailed study in which a variety of MC codes are intercompared. Also, a comparison with measurements done by using radiochromic-dye film, and an extrapolation chamber is carried out. Measured and calculated values were found to agree within 10% in a polystyrene phantom. On the other hand, the calculated depth dose curves, using the MC codes, were within 5% at 4 mm depth, after an adequate selection of the tracking parameters. In this last case water was considered the medium surrounding the source.

Here we have used the MC codes PENELOPE[15] and GEANT4.[16] PENELOPE was designed specifically to account for the transport of low-energy electrons, photons, and positrons, and has been used to simulate other brachytherapy sources.[17,18] GEANT4 includes special packages that permit us to describe low-energy physics processes and, at present, it is

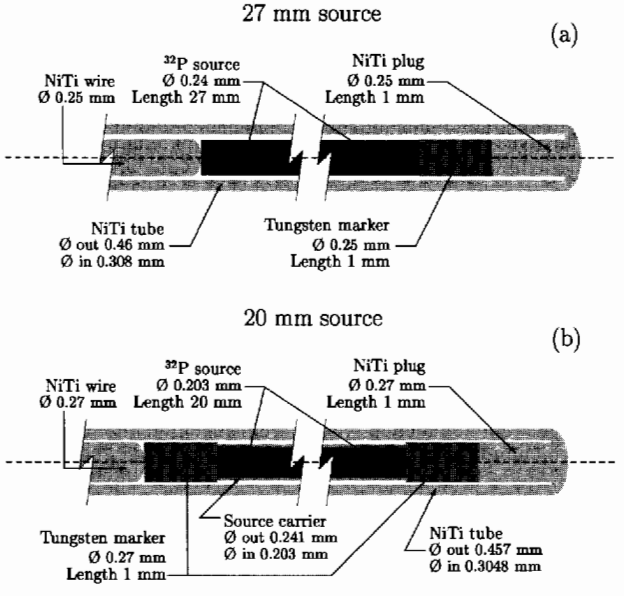

FIG. 1. Schematic view of the 27 (upper panel) and 20 mm (lower panel) ^{32}P sources manufactured by the Guidant Corporation.

being used to simulate different situations of medical physics interest.[16] In this work we have determined the dose rate at the reference point, the depth dose, and the two-dimensional dose distribution. We also calculated the radial dose and the anisotropy functions, as proposed in the adapted AAPM TG-60 formalism for cylindrical sources,[19] used also in Ref. 12. We compare some of our results with those quoted in Ref. 11.

II. MATERIAL AND METHODS

A. Source models

A schematic view of the geometry of the two sources analyzed is shown in Fig. 1. The 27 mm source has been described in Refs. 7, 8. The geometry of the 20 mm source has been obtained from Ref. 11 and corresponds closely to that quoted in Ref. 14. The active cores are cylinders with a length of 27 and 20 mm, respectively. These cores are made of $C_2H_6O_2$. The 20 mm source presents a 0.019 mm thick source carrier wrapping the active core. This is made of polymide. The cores are encapsulated by NiTi tubes with a thickness of 0.076 mm in both sources. In the 27 mm source, a tungsten x-ray marker of 1 mm in length follows the core at the distal end. In the case of the 20 mm source, two markers of the same characteristics are located at both the distal and the proximal ends of the active core. Both sources include a NiTi plug of 1 mm in length following the distal tungsten x-ray marker. A NiTi hemispherical seal is welded at the distal end and an unbound NiTi wire is attached to the proximal end in both sources. Empty regions between the different pieces and the capsules are supposed to be filled with air.

Sources are centered inside a catheter of Nylon-12. In some of the calculations done for the 27 mm source, we have considered a helicoidal catheter (labeled catheter 1) reported in Refs. 7–12. In the case of the 20 mm source, we have calculated using both this helicoidal catheter and a lobed catheter (labeled catheter 2) currently in use. This catheter is a new design to increase the blood flow during the procedure. Both catheters were modeled as tubes with an external radius of 0.4445 mm, while the inner diameter was 0.597 mm for catheter 1 and 0.5716 mm for catheter 2. Gaps between catheters and sources are assumed to be filled with air.

The catheter and source were placed in a water phantom the dimensions of which are large enough to ensure no significant loss of radiation.

The composition and density considered in the simulation for the different materials are given in Table I.

B. Monte Carlo calculations

In this work the PENELOPE[15] and GEANT4[16] Monte Carlo codes have been used to perform the simulations. PENELOPE is a general purpose MC code that allows us to simulate the coupled electron–photon transport. It can be applied to energies ranging from a few hundred eV up to 1 GeV and with arbitrary materials. Besides, PENELOPE permits a good description of the particle transport at interfaces and presents an accurate description of the electron transport at low energies. These characteristics make PENELOPE a useful tool for medical physics applications, as previous works have

TABLE I. Composition of the different materials used in the MC simulations performed in this work. The values correspond to the weight fraction of each element in the material. In the case of $C_2H_6O_2$, the density quoted is that used in the 20 mm source. For the 27 mm source a density of 1.12 g cm^{-3} has been used.

	$C_2H_6O_2$	NiTi	Tungsten	Polymide	Air	Nylon-12
H	0.097 432			0.026 362		0.117 49
C	0.387 026			0.691 133	0.000 124	0.730 45
N				0.073 270	0.755 267	0.070 98
O	0.515 542			0.209 235	0.231 781	0.081 08
Ar					0.012 827	
Ti		0.44				
Ni		0.56				
W			1.0			
Density [g cm^{-3}]	1.1155	6.5	19.3	1.096	0.001 204 8	1.196

pointed out (see, e.g., Refs. 17, 18). We have used the 2001 version of the code. Details about the physical processes included can be found in Ref. 15.

GEANT4 is a toolkit aiming to simulate the passage of particles through matter for applications in high-energy physics, nuclear experiments, medical physics studies, etc. Due to its purpose, the available energy range and the possible particles to be simulated are much larger than for PENELOPE. GEANT4 includes low-energy packages that extend the energy range of particle interactions for electrons, positrons, and photons down to 250 eV, and can be used up to approximately 100 GeV. In this work we have used the version 4.1 with the patch-01 and the low-energy package G4EMLOW1.1. Detailed documentation concerning the physics involved can be found in Ref. 16.

As the sources considered here present cylindrical symmetry, a cylindrical coordinate system was used with the origin in the center of the active core and with the z axis along the source and pointing to its distal end. The dose distributions were supposed to be functions of the axial coordinate z and the radial coordinate ρ. The position of the reference point is ($\rho_0=2$ mm, $z_0=0$).

The radionuclide was assumed to be uniformly distributed inside the active core. The direction of the emitted electrons was supposed to be isotropic around the initial position. The initial electron energies were sampled from the corresponding Fermi distributions, taken from Ref. 20. A calculated average energy of 0.6957 MeV was obtained, in agreement with values reported in previous works.[8,21]

In PENELOPE, analog simulation is performed for photons. For electrons, instead, the simulation is done in a mixed scheme in which collisions characterized by a scattering angle larger than a certain value are called hard collisions and are individually simulated, while collisions with a scattering angle smaller that the limit value are called soft collisions and are described by means of a multiple scattering theory. The electron tracking is controlled by means of four parameters. C_1 and C_2 refer to elastic collisions. C_1 gives the average angular deflection due to a elastic hard collision and to the soft collisions previous to it. C_2 represents the maximum value permitted for the average fractional energy loss in a step. On the other hand, W_{cc} and W_{cr} are energy cutoffs to distinguish hard and soft events. Thus, the inelastic electron collisions with energy loss $W<W_{cc}$ and the emission of bremsstrahlung photons with energy $W<W_{cr}$ are considered in the simulation as soft interactions. In our calculations the simulation parameters were fixed to the following values: $W_{cc}=5$ keV, $W_{cr}=1$ keV, $C_1=C_2=0.05$, $s_{max}=10^{35}$. This last parameter is an upper bound for the length of the steps generated in the simulation.

Photons were simulated down to 1 keV. Primary electrons, δ rays, and positrons were absorbed when they slow down to kinetic energies of 1 keV, in air, and 50 keV, in all the remaining materials, except in the active core, where the cutoff energy was fixed to 200 keV. This value takes care of the fact that electrons with such an energy are not expected to leave the active core. Those betas generated with energies below the simulation threshold were not transported and their energy was deposited at the source position.

In case of GEANT4 simulations, it is necessary to choose a given range threshold for each particle type. This threshold is converted, internally, to an energy threshold below which secondary particles are not emitted. In our calculations the range thresholds have been fixed to 100 nm providing energy thresholds of 1 keV for both photons and electrons in all materials considered.

The statistical uncertainties were calculated by scoring both the energy deposited in each voxel and its square for each history. These voxels were taken to be annular bins with thicknesses $\Delta\rho=0.1$ mm and $\Delta z=0.2$ mm. The average energy deposited in a given voxel (per incident particle) is

$$E_{\text{mean}}=\frac{1}{N}\sum_{i=1}^{N} e_i,$$

where N is the number of simulated histories and e_i is the energy deposited by all the particles of the ith history (that is, including the primary particle and all the secondaries it generates). The statistical uncertainty is given by

$$\sigma_{E_{\text{mean}}}=\sqrt{\frac{1}{N}\left[\frac{1}{N}\sum_{i=1}^{N} e_i^2-E_{\text{mean}}^2\right]}.$$

The uncertainties given throughout the paper correspond to 1σ. In tables, and in order to simplify the writing, they are given between parentheses; for example, a value quoted as 0.956(2) means 0.956 ± 0.002.

In case of the 27 mm source, the simulations have been done by following 2×10^7 histories for PENELOPE and 5×10^7 for GEANT4. For the 20 mm source, a total of 5×10^7 histories were simulated with both codes. These numbers permitted to keep the statistical uncertainties under reasonable levels.

Additionally, we performed, for the 20 mm source, simulations with PENELOPE by using scoring voxels given by cylindrical annuli of $\Delta z=13$ mm centered along the source axial direction, and $\Delta\rho=0.1$ mm in the radial direction. A total of 6×10^7 histories were followed in this case. These scoring voxels warranty radial distributions that are effectively constant over the axial length and permit the uncertainty to be reduced considerably.

III. RESULTS

A. 27 mm source

First we validated the MC codes with the old 27 mm source. Our results were compared with those reported in literature.

In Refs. 7 and 8, the MCNPv4B2 code was used. Mourtada *et al.*[7] transported 10^6 histories in each run, with scoring voxels given by cylindrical annuli of 20 mm in the source axial direction and 0.1 mm in the radial direction. They showed also the dose rate per unit activity along the transverse axis. The same code and voxels were used by Bohm *et al.*[8] for the dose rate per unit activity along the transverse axis. Besides, these authors calculated the dose to water, away and along the source, using thin cylindrical shells with

TABLE II. Two-dimensional dose rates (in cGy s^{-1} mCi^{-1}) for the 27 mm source sheathed by catheter 1. The errors corresponding to the calculations performed with MCNPv4B2 (Ref. 8) as well as those with EGSnrc and EGS4 (Ref. 12) are quoted to be below 1%. The CYLTRAN/ITS3 data have been obtained by scanning Fig. 11 of Ref. 11 and therefore are indicative only.

z (mm)	ρ (mm)	This work		Ref. 8	Ref. 11	Ref. 12	
		PENELOPE	GEANT4	MCNPv4B2	CYLTRAN/ITS3	EGSnrc	EGS4
0.0	1.0	0.718(3)	0.721(2)	0.728	0.801	0.731	0.729
	2.0	0.221(1)	0.2379(9)	0.232	0.232	0.225	0.222
	3.0	0.0718(6)	0.0868(4)	0.0785	0.0767	0.0732	0.0708
	4.0	0.0202(3)	0.0281(2)	0.0229	0.0212	0.0207	0.0193
10.0	1.0	0.719(3)	0.717(2)	0.725			
	2.0	0.220(1)	0.2356(9)	0.230			
	3.0	0.0708(6)	0.0853(4)	0.0769			
	4.0	0.0206(3)	0.0275(2)	0.0223			
12.0	1.0	0.677(3)	0.667(2)	0.681			
	2.0	0.193(1)	0.2046(8)	0.202			
	3.0	0.0609(6)	0.0713(4)	0.0654			
	4.0	0.0167(3)	0.0230(2)	0.0186			
14.0	1.0	0.180(2)	0.187(1)	0.188			
	2.0	0.0755(8)	0.0816(5)	0.0793			
	3.0	0.0266(4)	0.0322(3)	0.0291			
	4.0	0.0076(2)	0.0109(1)	0.00870			
16.0	1.0	0.0097(5)	0.0130(3)	0.0113			
	2.0	0.0067(3)	0.0101(2)	0.008 58			
	3.0	0.0035(1)	0.0051(1)	0.004 23			
	4.0	0.001 11(7)	0.001 92(6)	0.001 35			

a thickness of 0.1 mm and a height of 0.1 mm as scoring voxels. Wang and Li[12] used scoring voxels equal to those we have considered here. Finally, Seltzer[11] quoted the results obtained for a simulation with CYLTRAN/ITS3, but did not give information about the scoring voxels.

The dose rate at the reference point for the unsheathed 27 mm source in water was calculated to be 0.215 ± 0.001 and 0.2312 ± 0.0008 cGy s^{-1} mCi^{-1} for PENELOPE and GEANT4, respectively, thus differing by 7%. These values must be compared with the results obtained with the other codes. The calculation with EGSnrc[12] provides 0.2185 ± 0.0002 cGy s^{-1} mCi^{-1}. Mourtada *et al.*[7] obtained 0.229 cGy s^{-1} mCi^{-1} by means of MCNPv4B2. Finally, in Ref. 8 a value of 0.232 ± 0.00028 cGy s^{-1} mCi^{-1} was found also with MCNPv4B2. This is the largest value found, which differs from the one we have obtained with PENELOPE (the smallest one) by ~8%.

In Table II we compare the dose rate per unit activity along the transverse axis (values for $z=0$ in the first set of rows) obtained with PENELOPE and GEANT4 with those of Refs. 8, 11, 12. The results correspond to the ^{32}P wire source sheathed by catheter 1. As we can see, PENELOPE produces results very similar to those of EGSnrc. In this case the differences for any ρ value are below 6% with respect to the dose rate obtained with PENELOPE at the reference point, $\dot{D}_{\mathrm{PEN}}(\rho_0,z_0)$. Up to $\rho=3$ mm, PENELOPE practically coincides with EGS4, the differences relative to $\dot{D}_{\mathrm{PEN}}(\rho_0,z_0)$ being smaller than 5%. The difference between GEANT4 (MCNPv4B2) and PENELOPE is below 8% (5%), relative to $\dot{D}_{\mathrm{PEN}}(\rho_0,z_0)$. In what respect to the results of CYLTRAN/ITS3, they show negligible differences with PENELOPE results. The fact that these last quoted values have been obtained by scanning Fig. 11 of Ref. 11 makes these differences only indicative.

TABLE III. Two-dimensional dose rates for the unsheathed 27 mm source. The values are normalized to the dose rate at the reference point ($\rho_0=2$ mm, $z_0=0$). The errors corresponding to the calculations performed with EGSnrc (Ref. 12) are quoted to be below 1%.

ρ (mm)	MC code	z (mm)				
		0.0	10.0	12.0	14.0	16.0
1.0	EGSnrc	3.2844	3.2730	3.0795	0.8230	0.0439
	PENELOPE	3.31(1)	3.29(1)	3.11(1)	0.835(8)	0.062(2)
	GEANT4	3.036(9)	3.023(9)	2.835(8)	0.789(5)	0.051(1)
2.0	EGSnrc	1.0000	0.9926	0.8762	0.3363	0.0324
	PENELOPE	1.000(6)	0.996(6)	0.881(6)	0.336(3)	0.039(1)
	GEANT4	1.000(4)	0.988(4)	0.860(3)	0.346(2)	0.0394(8)
3.0	EGSnrc	0.3226	0.3194	0.2711	0.1176	0.0158
	PENELOPE	0.323(3)	0.317(3)	0.271(3)	0.117(2)	0.0182(7)
	GEANT4	0.358(2)	0.352(2)	0.299(2)	0.131(1)	0.0209(5)
4.0	EGSnrc	0.0897	0.0890	0.0744	0.0336	0.0050
	PENELOPE	0.089(1)	0.091(1)	0.074(1)	0.0329(8)	0.0050(3)
	GEANT4	0.1153(9)	0.1125(9)	0.0957(8)	0.0453(6)	0.0079(2)

TABLE IV. Two-dimensional dose rates (in cGy s^{-1} mCi^{-1}) for the unsheathed 20 mm source in water, calculated with PENELOPE (first row) and GEANT4 (second row) for each z value. All the results have been obtained using voxels with $\Delta z = 0.2$ mm, except those of the first row corresponding to $z = 0$, which have been calculated with PENELOPE using voxels with $\Delta z = 13$ mm.

z (mm)	ρ (mm)									
	0.4	0.6	0.8	1.0	1.5	2.0	2.5	3.0	4.0	5.0
		$\Delta z = 13$ mm		0.9576(3)	0.5139(2)	0.2918(1)	0.166 89(9)	0.093 86(6)	0.026 18(3)	
0.0	2.771(6)	1.788(4)	1.279(3)	0.961(2)	0.512(1)	0.2908(9)	0.1667(6)	0.0936(4)	0.0263(2)	0.005 52(9)
	2.544(6)	1.730(4)	1.256(3)	0.952(2)	0.527(1)	0.311(1)	0.1877(7)	0.1133(5)	0.0364(3)	0.0091(1)
2.0	2.770(6)	1.790(4)	1.275(3)	0.956(2)	0.517(1)	0.2912(9)	0.1670(6)	0.0940(4)	0.0260(2)	0.005 61(9)
	2.542(6)	1.736(4)	1.259(3)	0.955(2)	0.526(1)	0.314(1)	0.1875(7)	0.1123(5)	0.0365(3)	0.0092(1)
4.0	2.771(6)	1.790(4)	1.274(3)	0.957(2)	0.514(1)	0.2899(9)	0.1673(6)	0.0937(4)	0.0263(2)	0.005 33(8)
	2.545(6)	1.727(4)	1.256(3)	0.947(2)	0.524(1)	0.310(1)	0.1873(7)	0.1129(5)	0.0362(3)	0.0091(1)
6.0	2.765(6)	1.786(4)	1.272(3)	0.952(2)	0.511(1)	0.2895(9)	0.1670(6)	0.0923(4)	0.0261(2)	0.005 52(9)
	2.549(6)	1.727(4)	1.258(3)	0.950(2)	0.525(1)	0.312(1)	0.1866(7)	0.1124(5)	0.0361(3)	0.0090(1)
7.0	2.761(6)	1.788(4)	1.267(3)	0.947(2)	0.507(1)	0.2866(9)	0.1635(6)	0.0920(4)	0.0253(2)	0.005 32(8)
	2.533(6)	1.719(4)	1.244(3)	0.938(2)	0.516(1)	0.305(1)	0.1819(7)	0.1092(5)	0.0347(2)	0.0087(1)
8.0	2.746(6)	1.761(4)	1.243(3)	0.929(2)	0.487(1)	0.2729(9)	0.1525(6)	0.0853(4)	0.0233(2)	0.004 79(8)
	2.507(6)	1.698(4)	1.223(3)	0.912(2)	0.495(1)	0.2870(9)	0.1712(7)	0.1008(5)	0.0319(2)	0.0079(1)
9.0	2.650(6)	1.663(4)	1.152(3)	0.839(2)	0.422(1)	0.2305(8)	0.1262(6)	0.0702(4)	0.0191(2)	0.003 97(7)
	2.410(6)	1.598(4)	1.122(3)	0.825(2)	0.427(1)	0.2421(9)	0.1407(6)	0.0827(4)	0.0261(2)	0.0066(1)
10.0	1.389(4)	0.891(3)	0.635(2)	0.471(2)	0.254(1)	0.1444(7)	0.0823(4)	0.0465(3)	0.0131(2)	0.002 68(6)
	1.271(4)	0.857(3)	0.620(2)	0.470(2)	0.261(1)	0.1541(7)	0.0940(5)	0.0557(3)	0.0181(2)	0.004 49(8)
11.0	0.086(1)	0.100(1)	0.1070(9)	0.1064(8)	0.0841(6)	0.0588(4)	0.0378(3)	0.0231(2)	0.0068(1)	0.001 39(4)
	0.094(1)	0.110(1)	0.114(1)	0.1132(9)	0.0924(6)	0.0668(5)	0.0457(3)	0.0291(3)	0.0100(1)	0.00247(6)

Two-dimensional dose distributions are shown in Tables II and III for some values of ρ and $z \geq 0$. Similar results are obtained for the negative values of z, though the source wire is not symmetric with respect to $z = 0$. In Table II our results are compared with those of Bohm *et al.*[8] calculated with MCNPv4B2 for the source sheathed by catheter 1. In Table III the dose distributions for the unsheathed source, normalized to the reference point, are compared with the results obtained by Wang and Li[12] using EGSnrc.

The differences between MCNPv4B2 and PENELOPE [see Table II], remain below 5%, relative to $\dot{D}_{\mathrm{PEN}}(\rho_0, z_0)$. The same situation appears for MCNPv4B2 and GEANT4, which give very similar results for $\rho < 2$ mm.

Table III shows that EGSnrc and PENELOPE provide very similar normalized doses. It is important to remember here that the difference in the doses at the reference point between both codes is 1.6% only. The differences maintain at more or less the same level for all z and ρ values studied.

Finally, and as we can see in both tables, the discrepancies between PENELOPE and GEANT4, observed for the dose rate per unit activity along the transverse axis, show up again. In any case the differences remain below 8% with respect to $\dot{D}_{\mathrm{PEN}}(\rho_0, z_0)$.

B. 20 mm source

1. Unsheathed source

Once we have analyzed the results obtained for the 27 mm source, we will discuss the dose rates found for the 20 mm source. All the results here correspond to the unsheathed source. For clarity, we leave the analysis of the sheathed source for the next subsection.

In Table IV (box labeled $z = 0$) we show the results we have obtained for the dose rate per unit activity along the transverse axis. The first row gives the results obtained using PENELOPE for voxels with $\Delta z = 13$ mm. The second (third) rows correspond to the results obtained with PENELOPE (GEANT4) for voxels with $\Delta z = 0.2$ mm. The dose rates at the reference point calculated with PENELOPE are 0.2918

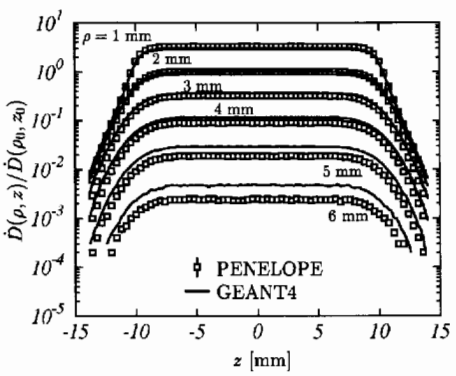

FIG. 2. Axial dose distributions for the unsheathed 20 mm source in water, for $\rho = 1$–6 mm. The values are normalized to the reference point ($\rho_0 = 2$ mm, $z_0 = 0$). PENELOPE results are plotted with points, while curves correspond to GEANT4.

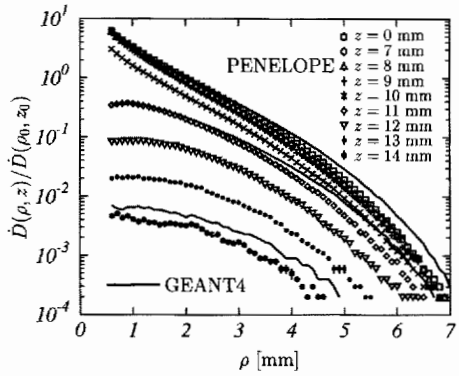

FIG. 3. Radial dose distributions for the unsheathed 20 mm source in water, for $z=0$ and $z=7-14$ mm. The values are normalized to the reference point ($\rho_0=2$ mm, $z_0=0$). PENELOPE results are plotted with points. GEANT4 results corresponding to $z=0$, 11, and 14 mm are plotted with lines.

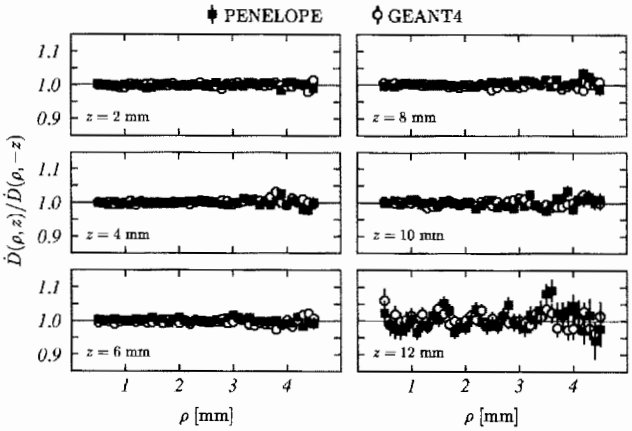

FIG. 4. Ratio of the dose at different z values to the dose at $-z$ as a function of ρ, for the unsheathed 20 mm source in water. PENELOPE (black squares) and GEANT4 (open circles) results are shown.

± 0.0001 cGy s^{-1} mCi^{-1} when the large scoring voxel (that with $\Delta z=13$ mm) is used and 0.2908 ± 0.0009 cGy s^{-1} mCi^{-1} for the small one (that with $\Delta z=0.2$ mm). GEANT4 produces a value of 0.311 ± 0.001 cGy s^{-1} mCi^{-1}, which differs from the previous ones in ~7%. On the other hand, the discrepancy between the results obtained with both codes increases with increasing ρ, showing a behavior similar to that found for the 27 mm source.

Figure 2 shows the comparison of the axial dose distributions (normalized to the corresponding reference points) obtained with both codes for ρ values ranging from 1 to 6 mm. The disagreement between PENELOPE and GEANT4 also shows up in Fig. 3. Therein the dose distributions along transverse axes (normalized to the reference point) for z values ranging from 7 to 14 mm are compared to those corresponding to $z=0$ mm. PENELOPE results are plotted with symbols, while GEANT4 calculations are only shown (curves) for $z=0$, 11, and 14 mm. For a given ρ value the discrepancy grows with z. In general, GEANT4 predicts larger doses at large ρ values. The case of the $z=11$ mm curve is a clear example of this behavior: up to $\rho\sim3$ mm both results are in a reasonable agreement, but for $\rho\geqslant5$ mm the GEANT4 result coincides with the PENELOPE one obtained for $z=10$ mm.

In the case of the 27 mm source, Wang and Li[12] quoted an asymmetry of the dose distribution due to the presence of the distal tungsten x-ray marker. Such asymmetry showed up for $z>13$ mm and the dose rates at the proximal and distal ends showed a relative difference below 25%. If this is so, the presence of two such markers, in the 20 mm source, should make this asymmetry disappear. Figure 4 shows the ratio of the dose at various z values to the dose at $-z$. The results are similar in both codes. As we can see, the ratio of the dose rates does not show statistically significant differences from unity, even at large z. This means that the asymmetry of the source structure due to the small differences between the distal and the proximal ends is smaller than statistical uncertainties and would therefore probably be irrelevant in practice.

In Fig. 5 we analyze the axial dose uniformity by plotting the ratio of the dose at $z=3$ up to 8 mm to the dose at $z=0$ as a function of ρ. The results show that, for a given ρ value, doses stay constant for axial positions up to 6–7 mm. This occurs for both PENELOPE and GEANT4 and means that the scoring voxels with $\Delta z=13$ mm, considered above to reduce the uncertainty in calculating the radial dose, can be used safely for that purpose.

The two-dimensional dose rates we have obtained using voxels with $\Delta z=0.2$ mm are listed in Table IV. For each z value, the first row corresponds to PENELOPE and the second one to GEANT4. The values for $z<0$ are not included because of the symmetry with respect to the corresponding $z>0$ results. On the other hand, the uniformity up to $z\sim6$ mm is again evident. The comparison between both codes indicates that GEANT4 predicts larger doses than PENELOPE, except for ρ below 0.5 mm.

To finish with the analysis of the unsheathed source, we calculated the radial dose functions and the anisotropy functions. Following Ref. 19, these quantities are given in the cylindrical coordinate system instead of the spherical one used in the TG-60 formalism.[5] For the radial dose we have

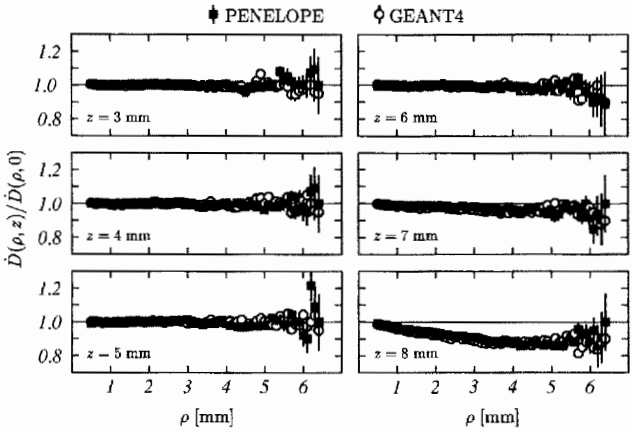

FIG. 5. Ratio of the dose at different z values to the dose at $z=0$ as a function of ρ, for the unsheathed 20 mm source in water. Results obtained with PENELOPE (GEANT4) are shown with black squares (open circles).

TABLE V. Radial dose functions for the ^{32}P sources. Simulations were performed in water.

ρ (mm)	20 mm source		27 mm source	
	PENELOPE	GEANT4	PENELOPE	EGSnrc
0.5	1.698(7)	1.507(6)	1.75(1)	1.7410
1.0	1.542(7)	1.428(6)	1.57(1)	1.5582
1.5	1.275(6)	1.226(6)	1.30(1)	1.2867
2.0	1.000(5)	1.000(5)	1.000(9)	1.0000
2.5	0.742(4)	0.780(4)	0.730(7)	0.7343
3.0	0.518(3)	0.586(3)	0.511(5)	0.5093
3.5	0.342(2)	0.412(3)	0.334(4)	0.3310
4.0	0.208(2)	0.270(2)	0.199(3)	0.1990
4.5	0.119(1)	0.167(2)	0.108(2)	0.1098
5.0	0.059(1)	0.090(1)	0.054(2)	0.0543
5.5	0.0257(6)	0.0451(9)	0.025(1)	0.0231
6.0	0.0099(4)	0.0190(6)	0.0093(7)	0.0083
6.5	0.0028(2)	0.0070(3)	0.0034(4)	0.0025
7.0	0.0006(1)	0.0017(2)	0.0008(2)	0.0007

$$g(\rho)=\frac{\dot{D}(\rho,z_0)}{\dot{D}(\rho_0,z_0)}\frac{G(\rho_0,z_0)}{G(\rho,z_0)}. \quad (1)$$

The anisotropy function is given by

$$F(\rho,z)=\frac{\dot{D}(\rho,z)}{\dot{D}(\rho,z_0)}\frac{G(\rho,z_0)}{G(\rho,z)}, \quad (2)$$

where $G(\rho,z)=\beta/(L\rho)$, with $L=27$ or 20 mm, according to the source considered, and β is the angle between the lines joining the point (ρ,z) and the two extremes of L.

Calculated radial dose functions for PENELOPE and GEANT4 in water are shown in Table V. As we can see, the discrepancies observed between both codes in previous results are evident here again. Besides, we have included the results obtained with PENELOPE for the 27 mm source and those quoted by Wang and Li for EGSnrc.[12] The radial dose function for the 20 mm source appears to be rather similar to that of the 27 mm source. The results obtained with PENELOPE differs less than 10% up to $\rho=6$ mm. Finally, PENELOPE and EGSnrc provide results that coincide within the statistical uncertainties for the 27 mm source.

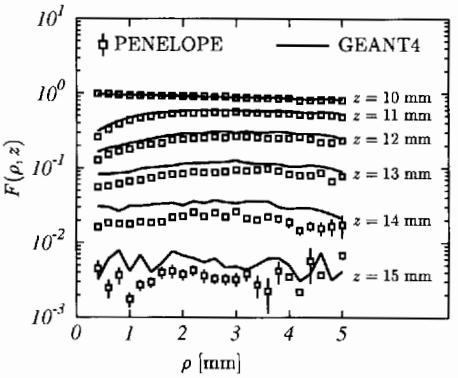

FIG. 6. A comparison between the anisotropy functions for the unsheathed 20 mm source obtained with PENELOPE (squares) and GEANT4 (curves). The errors for GEANT4 results are of the same order than those obtained with PENELOPE.

Table VI shows the anisotropy function calculated for the unsheathed 20 mm source with PENELOPE. These results are compared in Fig. 6 with those obtained with GEANT4. As in previous comparisons, the discrepancies between both codes appear to be noticeable for large ρ and/or z values, though the absolute differences remain small in comparison with the values obtained at the reference point.

2. Sheathed source

Here we analyze the effect of the catheter on the dosimetry. First we compare the results we have obtained with both codes with the scarce data available in the literature. Table VII shows this comparison with the data provided by the manufacturer in the source manual (second column) and with the results of a set of calculations with different codes performed by Seltzer.[11] In these calculations the scoring voxels were taken to be annuli of radial thickness 0.1 mm and axial length 15 mm, centered along the active wire length. This produces greatly reduced statistical uncertainties. As can be seen, our results for PENELOPE coincide with those found with CYLTRAN/ITS3 and PENELOPE in Ref. 11, except for small deviations (less than 1%) at $\rho=2$ mm in the last case.

TABLE VI. Anisotropy function $F(\rho,z)$ for the unsheathed 20 mm source in water, calculated with PENELOPE.

z (mm)	ρ (mm)									
	0.4	0.6	0.8	1.0	1.5	2.0	2.5	3.0	4.0	5.0
0.0	1.000(3)	1.000(3)	1.000(3)	1.000(4)	1.000(4)	1.000(5)	1.000(6)	1.000(7)	1.00(1)	1.00(2)
2.0	1.001(3)	1.003(3)	0.999(3)	0.998(4)	1.014(4)	1.007(5)	1.009(6)	1.012(7)	1.00(1)	1.03(2)
4.0	1.005(3)	1.009(3)	1.006(3)	1.009(4)	1.024(4)	1.022(5)	1.035(6)	1.038(7)	1.05(1)	1.02(2)
6.0	1.013(3)	1.022(3)	1.025(4)	1.028(4)	1.055(4)	1.071(5)	1.094(6)	1.091(8)	1.12(1)	1.14(3)
7.0	1.022(3)	1.039(3)	1.042(4)	1.050(4)	1.087(4)	1.111(5)	1.130(6)	1.153(8)	1.16(1)	1.17(3)
8.0	1.038(3)	1.057(3)	1.067(4)	1.084(4)	1.122(5)	1.148(5)	1.151(7)	1.169(8)	1.16(1)	1.14(3)
9.0	1.068(3)	1.094(4)	1.108(4)	1.115(4)	1.128(5)	1.128(6)	1.102(7)	1.106(8)	1.08(1)	1.05(3)
10.0	0.990(4)	0.977(4)	0.967(4)	0.949(4)	0.944(5)	0.927(5)	0.905(6)	0.894(7)	0.87(1)	0.81(2)
11.0	0.261(4)	0.331(4)	0.392(4)	0.441(4)	0.512(4)	0.548(5)	0.561(5)	0.569(6)	0.542(9)	0.49(2)
12.0	0.128(4)	0.153(3)	0.168(3)	0.179(3)	0.218(3)	0.246(4)	0.260(4)	0.269(4)	0.250(6)	0.24(1)
13.0	0.056(3)	0.057(2)	0.061(2)	0.067(2)	0.077(2)	0.086(2)	0.089(2)	0.095(3)	0.084(4)	0.079(5)
14.0	0.016(2)	0.018(2)	0.018(1)	0.018(1)	0.018(1)	0.023(1)	0.023(1)	0.026(2)	0.019(3)	0.017(6)
15.0	0.005(1)	0.0025(7)	0.0037(9)	0.0018(4)	0.0034(7)	0.0038(6)	0.0031(4)	0.0032(6)	0.00351(3)	0.0068(1)

TABLE VII. Depth doses (in cGy s^{-1} mCi^{-1}) for the 20 mm source sheathed by catheter 1. The values of the second column are those provided by the manufacturer in the GALILEO™ system manual. Simulations were performed in water.

ρ		Ref. 11					This work	
[mm]	Guidant	CYLTRAN/ITS3	MCNP4C	EGS4	EGSnrc	PENELOPE	PENELOPE	GEANT4
1.0	0.999						0.975(2)	0.971(2)
1.5	0.548						0.526(1)	0.540(1)
2.0	0.317	0.300	0.314	0.296	0.296	0.298	0.3005(9)	0.321(1)
2.5	0.184						0.1723(6)	0.1957(7)
3.0	0.105						0.0976(4)	0.1172(5)
3.5	0.0569						0.0534(3)	0.0683(4)
4.0	0.0290	0.0276	0.0285	0.0255	0.0254	0.0274	0.0274(2)	0.0384(3)
4.5	0.0135						0.0133(1)	0.0200(2)

The values provided by Guidant are between 5% and 10% above those we have found for PENELOPE. MCNP4C results are similar to the Guidant ones, and those calculated with EGS4 and EGSnrc fall to ~7% below those obtained with PENELOPE at ρ=4 mm. The values found with GEANT4 follow the same trend seen in the previous sections.

Figure 7 shows the relative difference

$$\frac{\dot{D}_{\text{cath}}(\rho,z_0)-\dot{D}(\rho,z_0)}{\dot{D}(\rho,z_0)}, \tag{3}$$

between the depth doses calculated with and without a catheter for PENELOPE (squares) and GEANT4 (disks). The results corresponding to the 20 mm source are shown. As we can see, both codes produce similar results with both catheters. However, GEANT4 shows an increase of the effect of the catheter above ρ=3.5 mm that is not present in the PENELOPE calculation. Similar results are obtained for the 27 mm source sheathed by catheter 1. On the other hand, catheter 2 produces a modification of the dose in water slightly smaller than catheter 1. This gives rise to enhancements of the dose rate on the transverse axis reaching ~4% above ρ=3 mm, while the first one increases the dose rate by ~2.5%, at most. This result is reasonable if one considers that catheter 2 has a smaller inner radius than catheter 1, thus reducing the air gap. In any case, uncertainties in source strength measurements might outweigh this correction in clinical practice.

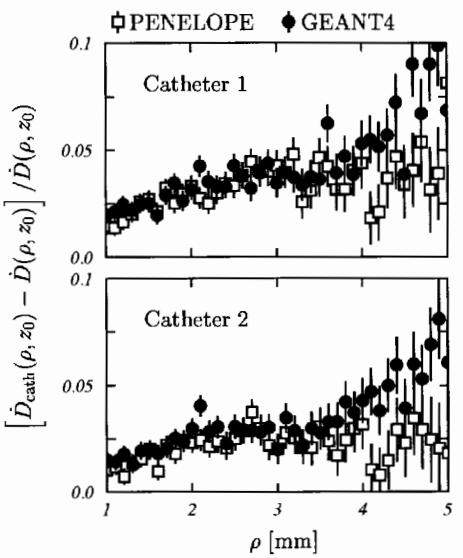

FIG. 7. The relative difference between the depth dose rates calculated for the 20 mm source sheathed, $\dot{D}_{\text{cath}}(\rho,z_0)$, and unsheathed, $\dot{D}(\rho,z_0)$, with PENELOPE (squares) and GEANT4 (disks). Upper (lower) panel corresponds to catheter 1 (2).

IV. CONCLUSIONS

In this work we have performed the dosimetric characterization of two wire sources of ^{32}P (of 27 and 20 mm active length) manufactured by the Guidant Corporation and clinically used in intravascular brachytherapy. To do so we have used the Monte Carlo codes PENELOPE and GEANT4.

First we have validated the codes by comparing the results obtained with these two codes with those available in the literature for the 27 mm source. The main conclusion is that PENELOPE produces dose rates in reasonable agreement with those quoted in Ref. 12 for EGSnrc and EGS4, except in the tails of the axial doses (large z values). Calculations performed with MCNPv4B2[7,8] differ from those obtained with PENELOPE as the distance to the source increases. The comparison between PENELOPE and GEANT4 shows a clear disagreement.

For the 20 mm source, we have calculated the depth doses on the transverse axis, the two-dimensional dose rate table, and the radial dose and anisotropy functions (these two according to the approach proposed in Ref. 19 for cylindrical sources). We have checked that the dose distribution remains uniform along the axial direction for $|z|$ smaller than 6–7 mm and ρ~7 mm. Besides, we have tested the symmetry of the dose distribution. The dose rates calculated with PENELOPE show a good agreement with the scarce data available, while those obtained with GEANT4 follow a trend similar to that observed in the 27 mm source.

The presence of the catheter sheathing the sources produces an increase in the dose rate on the transverse axis. This enhancement is larger for the helicoidal catheter (catheter 1) than for the lobed one (catheter 2). For the first one, the dose on the transverse axis increases up to 4% above ρ=3 mm, while the second one produces a maximum enhancement of

~2.5%. These differences could produce non-negligible modifications in the clinical use of the sources.

The results we have obtained indicate that PENELOPE produces a dose rate map that can be considered to represent the dosimetric characterization of the sources studied here. The appreciable discrepancies shown by GEANT4 results need a deeper investigation in order to clarify the origin of these differences. In particular, to determine if they are due to the physics included in the simulations or to the tracking procedure should be of great interest. We are working in this direction.

The full dataset we have obtained here is available at http://fm131.ugr.es/P32-IVB.

ACKNOWLEDGMENTS

The authors wish to acknowledge the Guidant Corporation (European division) for the assistance provided concerning the geometrical details of the sources investigated here. We are also indebted to Dr. Jenkins (Guidant, Texas) for his patient answering of our questions. This work has been supported in part by the Junta de Andalucía (FQM0225).

[a]Electronic mail: lallena@ugr.es

[1] S. J. Pocock *et al.*, "Meta analysis of randomized trials comparing coronary angioplasty with bypass surgery," Lancet **346**, 1184–1189 (1995).

[2] R. A. Fox, "Intravascular brachytherapy of the coronary arteries," Phys. Med. Biol. **47**, R1–R30 (2002).

[3] A. E. Raizner, G. L. Kaluza, and N. M. Ali, "Clinical experience with a spiral balloon centering catheter for the delivery of intracoronary radiation therapy," Cardiovasc. Radiat. Med. **1**, 214–219 (1999).

[4] R. Waksman, A. Raizner, A. J. Lansky, A. C. Yeung, L. J. Vandertie, and P. S. Teirstein, "Beta-radiation to INHIBIT recurrence of in-stent restenosis: Clinical and angiographic results of the multicenter, randomized, doubly blind study," Circulation **102**, e9046 (2000).

[5] R. Nath *et al.*, "Intravascular brachytherapy physics. Report of the AAPM Radiation Therapy Comittee Task Group No. 60," Med. Phys. **26**, 119–152 (1999).

[6] R. Pötter *et al.*, "Recommendations of the EVA GEC ESTRO Working Group: prescribing, recording and reporting in endovascular brachytherapy. Quality assurance, equipment, personnel and education," Radiother. Oncol. **59**, 339–360 (2001).

[7] F. A. Mourtada, C. G. Soares, S. M. Seltzer, and S. H. Lott, "Dosimetry characterization of ^{32}P catheter-based vascular brachytherapy source wire," Med. Phys. **27**, 1770–1776 (2000).

[8] T. D. Bohm, F. A. Mourtada, and R. K. Das, "Dose rate table for a ^{32}P intravascular brachytherapy source from Monte Carlo calculations," Med. Phys. **28**, 1770–1775 (2001).

[9] M. Todorovic, F. Cremers, D. Albers, and R. Schmidt, "Simulation of a ^{32}P sourcewire and a ^{90}Sr/^{90}Y sourcetrain using MCNP4B and EGS4," in *Advanced Monte Carlo for Radiation Physics, Particle Transport Simulations and Applications*, Proceedings of the Monte Carlo 2000 Conference, edited by A. Kling, F. Barão, M. Nakagawa, L. Távora, and P. Vaz (Springer-Verlag, Berlin, 2001).

[10] V. Sehgal, Z. Li, J. R. Palta, and W. E. Bolch, "Dosimetric effect of source centering and residual plaque for β-emitting catheter based intravascular brachytherapy sources," Med. Phys. **28**, 2162–2170 (2001).

[11] S. M. Seltzer, "Monte Carlo modeling for intravascular brachytherapy sources," NISTIR 6871, NIST Technical Publ., 2002.

[12] R. Wang and X. A. Li, "Monte Carlo characterization of a ^{32}P source for intravascular brachytherapy," Med. Phys. **28**, 1776–1785 (2001).

[13] X. A. Li and R. Shih, "Dose effects of guide wires for catheter-based intravascular brachytherapy," Int. J. Radiat. Oncol., Biol., Phys. **51**, 1103–1110 (2001).

[14] F. Mourtada, C. G. Soares, S. M. Seltzer, P. M. Bergstrom, J. M. Fernández-Varea, J. Asenjo, and S. H. Lott, "Dosimetry characterization of a ^{32}P source wire used for intravascular brachytherapy with automated stepping," Med. Phys. **30**, 959–971 (2003).

[15] F. Salvat, J. M. Fernández-Varea, E. Acosta, and J. Sempau, "PENELOPE, a code system for Monte Carlo simulation of electron and photon transport," NEA-OECD, Paris, 2001.

[16] S. Agostinelli *et al.*, "GEANT4—a simulation toolkit," Nucl. Instrum. Methods Phys. Res. A **506**, 250–303 (2003).

[17] A. Sánchez-Reyes, J. J. Tello, B. Guix, and F. Salvat, "Monte Carlo calculation of the dose distributions of two ^{106}Ru eye applicators," Radiother. Oncol. **49**, 191–196 (1998).

[18] J. Asenjo, J. M. Fernández-Varea, and A. Sánchez-Reyes, "Characterization of a high-dose rate ^{90}Sr–^{90}Y source for intravascular brachytherapy by using the Monte Carlo code PENELOPE," Phys. Med. Biol. **47**, 697–711 (2002).

[19] D. R. Schaart, M. C. Clarijs, and A. J. J. Bos, "On the applicability of the AAPM TG-60/TG-43 dose calculation formalism: Proposal for an adapted formalism," Med. Phys. **28**, 638–653 (2001).

[20] E. García-Toraño and A. Grau Malonda, "EFFY, a new program to compute the counting efficiency of beta particles in liquid scintillators," Comput. Phys. Commun. **36**, 307–312 (1985).

[21] S. Vynckier and A. Wambersie, "Dosimetry of beta sources in radiotherapy I. The beta point source dose function," Phys. Med. Biol. **27**, 1339–1347 (1982).